

Radiative analysis of entropy generation on MHD Walters-B fluid with heat and mass transfer

S. Asad

Department of Mathematics, College of Science, Majmaah University, Al-Majmaah, 11952, Saudi Arabia

Received: March 01, 2021, Revised: May 31, 2021

Boundary layer flow of Walters-B liquid by an inclined unsteady stretching sheet was investigated. Simultaneous effects of heat and mass transfer on entropy generation were considered. Analysis was carried out in the presence of thermal radiation and viscous dissipation. Convective condition was employed for the heat transfer process. Resulting problems were computed for the convergent solutions of velocity, temperature and concentration fields. The effects of different physical parameters on entropy generation, velocity, temperature and concentration fields are discussed. It was observed that angle of inclination and Weissenberg number decay the velocity field whereas the velocity field is an increasing function of mixed convection parameter. Temperature field rises for larger values of Eckert number and Biot number. The concentration field decreases when Sc increases. Numerical values of skin friction coefficient, local Nusselt number and local Sherwood number were computed and analyzed. We concluded from Table 1 that the magnitude of skin friction coefficient decays for larger values of mixed convection parameter, radiation parameter and Eckert number. Entropy generation decreases when temperature/parameter ratio increases while magnetic parameter boosts the entropy generation. It was also noted that entropy generation rises with larger Reynolds numbers.

Keywords: MHD Walters-B fluid, entropy generation, viscous dissipation, thermal radiation, unsteady inclined stretching sheet, convective boundary condition.

INTRODUCTION

It is a commonly accepted argument now that the fluids in numerous technological and biological applications do not follow the commonly assumed relationship between the stress and the rate of strain at a point. Such fluids have come to be known as non-Newtonian fluids. Materials like molten plastics, polymers, shampoos, certain oils, personal care products, pulps, mud, ice, foods and fossil fuels, which may saturate in underground beds, display non-Newtonian behavior. In recent times, there has been a great deal of interest in understanding the behavior of viscoelastic fluids. Such fluids are of great interest to the applied mathematicians and engineers, essentially from the points of view of theory and simulation of differential equations. On the other hand, in applied sciences such as rheology or physics of the atmosphere, the approach to fluid mechanics is in an experimental set up leading to the measurement of material coefficients. In theoretically studying how to predict the weather, the ordinary differential equations represent the main tool. Since the failures in the predictions are strictly related to a chaotic behavior, one may find it unessential to ask whether the fluids are really Newtonian. Constitutive equations describe the rheological properties of

viscoelastic fluids. Most of the models or constitutive equations are empirical or semi-empirical. Also the extra rheological parameters in such relations add more nonlinear terms to the corresponding differential systems. The order of the differential systems involving non-Newtonian fluids is higher in general than the Navier-Stokes equations. In view of all these challenges there is paucity of approximate, analytic and numerical solutions of the nonlinear flow problems of viscoelastic fluids. Keeping this in view, the various investigators are still developing such solutions (see [1-10] and some relevant papers therein).

No doubt, there have been significant advances in the mathematical modeling and analysis of steady boundary layer flows of non-Newtonian fluids over a stretching surface with/without heat and mass transfer. Such flow analysis in presence of heat transfer is important in polymer extrusion, paper production, continuous casting, cooling of metallic plates in a bath, etc. Further, not much attention in this direction is focused on the unsteady flow of MHD non-Newtonian fluids with entropy generation over a stretching sheet. Hayat *et al.* [11] investigated the unsteady flow with heat and mass transfer characteristics in a third-grade fluid bounded by a stretching sheet. They found a series of solutions of the problem.

To whom all correspondence should be sent:
E-mail: asadsadia@ymail.com

Flow of Maxwell fluid over a stretching surface in the presence of a first-order constructive/destructive chemical reaction has been reported by Mukhopadhyay and Bhattacharyya [12]. Mukhopadhyay [13] studied the unsteady two-dimensional flow of a non-Newtonian fluid over a stretching surface with prescribed surface temperature. The heat transfer in unsteady boundary layer stagnation-point flow over a shrinking/stretching sheet is investigated by Bhattacharyya [14]. Mishra and Singh [15] investigated the fluid flow along a vertical unsteady stretching sheet with a combined effect of heat and mass transfer. They formulated the problem in the presence of heat generation and a transverse magnetic field.

In this study, we focus on entropy generation, heat and mass transfer, with MHD non-Newtonian fluid. Heat and mass transfer are some of the most interactive factors of energy consumption. Entropy generation in a magnetohydrodynamic flow of non-Newtonian fluid is an efficient method for enhancing the heat transfer, which is very useful to enhance the performance of industrial processing. Initially the concept of entropy generation minimization is given by Bejan [16, 17]. After that many researchers discuss this concept with different physical aspects and different fluid models. Effect of entropy generation on the convective MHD flow of a third-grade fluid is investigated by Rashidi *et al.* [18]. They discussed influences of different physical parameters on the entropy generation. Sithole *et al.* [19] studied a nano fluid flow with entropy generation and nonlinear thermal radiation. They focused on the effects of nonlinear radiation on entropy generation. Naz *et al.* [20] analyzed the cross nanofluid with entropy generation and gyrostatic motile microorganisms. They observed that Brownian motion parameter and temperature difference parameter play an important role to control the concentration of nano particles and the process of entropy generation, respectively.

The purpose of the present investigation is to examine the effect of entropy generation on the boundary layer flow of MHD Walters-B liquid over an unsteady inclined stretching sheet. Simultaneous effects of heat and mass transfer are taken into account. Energy equation in presence of viscous dissipation and thermal radiation effects is considered. Resulting nonlinear problems are formulated first and then solved for the convergent solutions. Contributions of involved parameters on the flow, temperature, concentration and entropy generation are examined. Skin friction coefficient

and Nusselt number are computed and analyzed.

Problem formulation

Here we investigate the flow of an incompressible Walters' B fluid due to an inclined stretching sheet with convective boundary condition. The effects of viscous dissipation and thermal radiation are present. The sheet is inclined at an angle α with the horizontal axis, i.e. x-axis and y-axis is taken normal to it. The extra stress tensor S in Walters' B fluid is given by:

$$S = 2\eta_0 A_1 - 2k_0 \frac{DA_1}{Dt}, \quad (1)$$

$$\frac{DA_1}{Dt} = \frac{\partial A_1}{\partial t} + V \cdot \nabla A_1 - A_1 \cdot \nabla V - (\nabla V)^T \cdot A_1. \quad (2)$$

In the above equations A_1 is the rate of strain tensor, $\frac{DA_1}{Dt}$ is the covariant derivative of the rate of strain tensor in relation to the material in motion and η_0 and k_0 denote the limiting viscosity at small shear rates and a short memory coefficient, respectively, i.e. :

$$\eta_0 = \int_0^\infty N(\tau) d\tau, \quad (3)$$

$$k_0 = \int_0^\infty \tau N(\tau) d\tau, \quad (4)$$

where $N(\tau)$ is the distribution function with relaxation time τ . Taking short memory into account the terms involving

$$\int_0^\infty \tau^n N(\tau) d\tau, \quad n \geq 2, \quad (5)$$

are neglected in case of Walter's B fluid [11]. The subjected boundary layer equations are given by:

$$\frac{\partial u}{\partial x} + \frac{\partial v}{\partial y} = 0, \quad (6)$$

$$\frac{\partial u}{\partial t} + u \frac{\partial u}{\partial x} + v \frac{\partial u}{\partial y} = \frac{\eta_0}{\rho} \left(\frac{\partial^2 u}{\partial y^2} \right) - \frac{k_0}{\rho} \left[\frac{\partial^3 u}{\partial t \partial y^2} + u \frac{\partial^3 u}{\partial x \partial y^2} + v \frac{\partial^3 u}{\partial y^3} + \frac{\partial u}{\partial x} \frac{\partial^2 u}{\partial y^2} \right] + g_0 \beta_T (T - T_\infty) \cos \alpha - \frac{\sigma B_0 u}{\rho}, \quad (7)$$

$$\rho c_p \left(\frac{\partial T}{\partial t} + u \frac{\partial T}{\partial x} + v \frac{\partial T}{\partial y} \right) = k \frac{\partial^2 T}{\partial y^2} - \frac{\partial q_r}{\partial y} + \eta_0 \left(\frac{\partial u}{\partial y} \right)^2 - 2k_0 \left[\frac{\partial u}{\partial y} \frac{\partial^2 u}{\partial t \partial y} + u \frac{\partial u}{\partial y} \frac{\partial^2 u}{\partial x \partial y} + v \frac{\partial u}{\partial y} \frac{\partial^2 u}{\partial y^2} \right] + \sigma B_0 u^2, \quad (8)$$

$$\frac{\partial C}{\partial t} + u \frac{\partial C}{\partial x} + v \frac{\partial C}{\partial y} = De \frac{\partial^2 C}{\partial y^2}, \quad (9)$$

$$u = u_s(x), \quad v = 0, \quad -k \frac{\partial T}{\partial y} = h(T_f - T), \quad C = C_w \text{ at } y = 0, \quad (10)$$

$$u \rightarrow 0, \quad T \rightarrow T_\infty, \quad C \rightarrow C_\infty \text{ as } y \rightarrow \infty, \quad (11)$$

in which u and v represent the velocity components along and normal to the sheet, $u_s = \frac{bx}{1-at}$ is the velocity of the stretching sheet, T is the fluid temperature, $\nu = (\mu/\rho)$ is the kinematic viscosity, ρ is the density of the fluid, k is the thermal conductivity of the fluid, h is the convective heat

transfer coefficient, $T_f = T_\infty + T_{ref} \frac{bx^2}{2\nu} (1-at)^{-3/2}$ is the surface temperature, C is the concentration of fluid, D is the effective diffusion coefficient and $C_w = C_\infty + \frac{cx}{1-at}$ is the fluid concentration.

We introduce:

$$f'''' + ff'' - f'^2 + -\varepsilon \left(f' + \frac{1}{2} \eta f'' \right) + We \left[\varepsilon \left(2f'' + \frac{1}{2} \eta f^{iv} \right) + f''^2 - 2f'f''' + ff^{iv} \right] + G\theta \cos \alpha - Mf' = 0, \quad (13)$$

$$\left(1 + \frac{4}{3} R \right) \theta'' - Pr \left[\frac{1}{2} \varepsilon (3\theta + \eta \theta') - f\theta' + 2f'\theta \right] + Pr E_c f''^2 - Pr E_c We \frac{1}{2} \varepsilon (3f''^2 + \eta f'' f''') - Pr E_c We (f' f''^2 - f f'' f''') + Pr Ec M f'^2 = 0, \quad (14)$$

$$\varphi'' + Sc(f\varphi' - f'\varphi) - \varepsilon Sc \left(\varphi + \frac{1}{2} \eta \varphi' \right) = 0, \quad (15)$$

$$f = 0, f' = 1, \theta' = -Bi[1 - \theta(0)] \varphi = 1 \text{ at } \eta = 0, \quad (16)$$

$$f' \rightarrow 0, \theta \rightarrow 0 \varphi \rightarrow 0 \text{ at } \eta \rightarrow \infty. \quad (17)$$

Here $We = \frac{k_0 b}{\eta_0 (1-at)}$ is the Weissenberg number, $Pr = \frac{\nu}{\sigma}$ is the Prandtl number, $\varepsilon = \frac{b}{a}$ is the ratio parameter, $G = \frac{g_0 \beta_T (T_s - T_\infty) x^3 / \nu}{u_s^2 x^2 / \nu}$ is the mixed convection parameter, $E_c = \frac{u_s^2}{c_p (T_s - T_\infty)}$ is the Eckert number, $R = \frac{4\sigma^* T_\infty^3}{k k^*}$ is the radiation parameter, $M = \frac{\sigma B_0^2 (1-at)}{\rho b}$ $Bi = \frac{h}{k} \sqrt{\frac{\nu(1-at)}{b}}$ is the Biot number and $Sc = \frac{\nu}{D}$ is the Schmidt number.

The skin friction coefficient C_f , the local Nusselt number Nu_x and the local Sherwood number Sh can be expressed in the following forms:

$$C_f = \frac{\tau_w}{\frac{1}{2} \rho u_s^2}, Nu_x = \frac{xq_w}{k(T_s - T_\infty)}, Sh = \frac{\sqrt{x} M_w}{D_w (C_s - C_\infty)}, \quad (18)$$

Hence,

$$\tau_w = \mu_0 \left. \frac{\partial u}{\partial y} \right|_{y=0} - k_0 \left\{ \frac{\partial^2 u}{\partial t \partial y} + u \frac{\partial^2 u}{\partial x \partial y} - 2 \frac{\partial u}{\partial x} \frac{\partial u}{\partial y} + v \frac{\partial^2 u}{\partial y^2} \right\} \Bigg|_{y=0}, \quad (19)$$

Dimensionless forms of skin friction coefficient C_f , local Nusselt number Nu_x and local Sherwood number Sh can be represented by the relations:

$$\psi = x \left(\frac{vb}{1-at} \right)^{-1/2} f(\eta), \theta(\eta) = \frac{T-T_\infty}{T_s-T_\infty}, \varphi(\eta) = \frac{C-C_\infty}{C_s-C_\infty}, \eta = y \left(\frac{b}{\nu(1-at)} \right)^{1/2}, \quad (12)$$

and the velocity components $u = \frac{\partial \psi}{\partial y}, v = -\frac{\partial \psi}{\partial x}$,

where ψ is the stream function. Now Eq. (6) is identically satisfied and Eqs. (7-11) are reduced into the following forms:

$$C_f = 2(Re_x)^{-1/2} \left[(1 + 3We) f''(\eta) - We \varepsilon \frac{1}{2} (3f''(\eta) + \eta f''(\eta)) \right] \Bigg|_{\eta=0},$$

$$Nu/Re_x^{1/2} = -(1 + \frac{4}{3} R) \theta'(0) \quad Sh/Re_x^{1/2} = -\varphi'(0), \quad (20)$$

in which $(Re_x)^{-1/2} = \sqrt{\frac{\nu}{xu_s}}$.

Convergence of the homotopy solutions

It is well known that the convergence of series (37 - 39) depends on the auxiliary parameters \hbar_f , \hbar_θ and \hbar_ϕ . These parameters are useful to control and adjust the convergence of series solutions. In order to find the admissible values of \hbar_f , \hbar_θ and \hbar_ϕ the \hbar - curves of $f''(0)$, $\theta'(0)$ and $\phi'(0)$ are displayed. Figs. (1-3) depict that the range of admissible values of \hbar_f , \hbar_θ and \hbar_ϕ are $-1.25 \leq \hbar_f \leq -0.26$, $-1.23 \leq \hbar_\theta \leq -0.27$ and $-1.26 \leq \hbar_\phi \leq -0.4$. The series converge in the whole region of η when $\hbar_f = \hbar_\theta = -0.8$ and $\hbar_\phi = -0.9$. Table 1 displays the convergence of homotopy solutions for different orders of approximations. Tabulated values clearly indicate that the 25th order of approximations is enough for the convergent solutions.

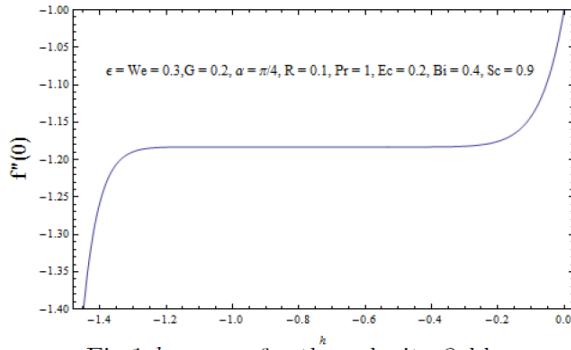


Fig.1 \tilde{h} -curve for the velocity field.

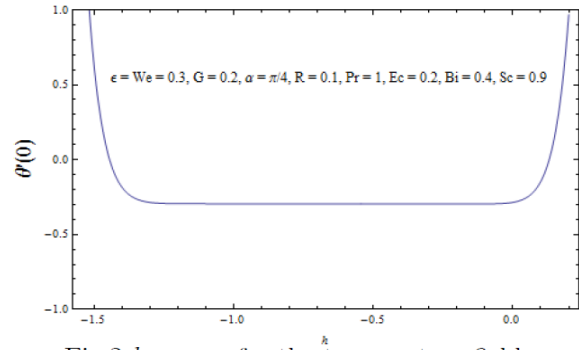


Fig.2 \tilde{h} -curve for the temperature field.

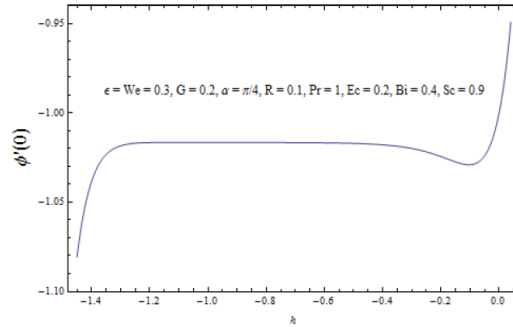


Fig.3 \tilde{h} -curve for the concentration field.

Entropy generation

This section discloses the influence of MHD Walter's B fluid with heat and mass transfer on entropy generation. Local volumetric rate of entropy generation is defined as:

$$S_{gen}''' = \frac{k}{T_\infty^2} \left[\left(\frac{\partial T}{\partial y} \right)^2 + \frac{16\sigma^* T_\infty^3}{3k^*} \left(\frac{\partial T}{\partial y} \right)^2 \right] + \frac{\sigma B_0^2 u^2}{T_\infty} + \frac{\mu}{T_\infty} \left[\left(\frac{\partial u}{\partial y} \right)^2 - 2k_0 \left\{ \frac{\partial u}{\partial y} \frac{\partial^2 u}{\partial t \partial y} + u \frac{\partial u}{\partial y} \frac{\partial^2 u}{\partial x \partial y} + v \frac{\partial u}{\partial y} \frac{\partial^2 u}{\partial y^2} \right\} \right]. \quad (21)$$

Above equation is the combination of three different phenomena. First is heat transfer, second due to magnetic field and third one is due to viscous dissipation of Walter's B fluid. Characteristic entropy generation rate is defined as:

$$\dot{S}_0''' = \frac{k(\Delta T)^2}{l^2 T_\infty^2}, \quad (22)$$

Thus, the dimensionless form of entropy generation is obtained by taking ratio of Eq. (21) and Eq. (22).

$$N_G = \frac{S_{gen}'''}{\dot{S}_0'''} = Re \left(1 + \frac{4}{3} R \right) \theta'^2 + \frac{1}{\theta_w'^2} Re Br (f''^2 + Mf'^2) - \frac{1}{\theta_w'^2} Re Br We \left[\frac{1}{2} \epsilon (3f''^2 + \eta f'' f''') + f' f''^2 - f f'' f''' \right]. \quad (23)$$

where $Re = \frac{u_s x}{\nu}$, $Br = \frac{\mu(u_s)^2}{k\Delta T}$ and $\theta_w' = \frac{\Delta T}{T_\infty}$.

GRAPHICAL RESULTS AND DISCUSSION

The arrangement of this section is to disclose the impact of different physical parameters, including ratio parameter, the Biot number, the Weissenberg

number, the Prandtl number, the Sherwood number, the Eckert number, the mixed convection parameter, the angle of inclination and the radiation parameter. The variation of aforementioned parameters is seen for the velocity, temperature and concentration fields. It is observed that the effects of α and ϵ on the velocity field are quite opposite (see Figs. 4 and 5). Velocity field and boundary layer thickness decay for larger values of α . The influence of Weissenberg number We on $f'(\eta)$ is shown in Fig. 6. Here the velocity field is a decreasing function of We . For large values of the mixed convection parameter G , the velocity field increases (see Fig. 7). Effects of radiation parameter R and Eckert number E_c are qualitatively similar for the velocity field $f'(\eta)$ (see Figs. 8 and 9). It is also noticed that the variation of R between 0 and 1 is insignificant on the temperature. Fig. 10 depicts the influence of ϵ on the temperature field. Apparently, both the temperature field and the thermal boundary layer thickness are decreased via ϵ . Fig. 11 gives the influence of Weissenberg number We on the temperature field. Here the temperature field is an increasing function of We . Fig. 12 shows that the temperature field decays very slowly when the mixed convection parameter G increases. Fig. 13 presents the influence of α on the temperature field. Both the temperature field and the thermal boundary layer thickness decrease when α increases. Fig. 14 witnesses that the temperature field is more pronounced when

radiation effects strengthen. Fig. 15 depicts the variation of Pr on temperature field. For larger values of the temperature and thermal boundary layer thickness it decreases. This is since enhancement in Pr causes a reduction in thermal conductivity. Effect of Eckert number Ec is displayed in Fig. 16. When we increase the Eckert number then the fluid kinetic energy increases and thus the temperature field increases for larger values of Eckert number. Fig. 17 shows the influence of Biot number on the temperature field. Larger Biot numbers correspond to more convection than conduction and this leads to an increase in temperature, as well as in thermal boundary layer thickness. Influence of parameter ϵ on the concentration field is displayed in Fig. 18. It is noticed that the concentration field decreases when ϵ is increased. Fig. 19 shows the influence of Weissenberg number We on the concentration field. It is clearly seen from this figure that the concentration field increases when the Weissenberg number We increases. Fig. 20 gives the influence of α on the concentration field. The angle of inclination α increases the concentration field. The effect of Sc on the concentration field is plotted in Fig. 21. The concentration field decreases when Sc increases. Here a larger Sc number corresponds to lower molecular diffusivity.

Deviation of entropy generation with η is depicted in Fig. 22 for different values of the radiation parameter. Increase in radiation parameter leads to an increase in entropy generation. It is also observed that near the surface variation is almost

negligible. Fig. 23 shows the dual behavior of the fluid parameter; small increment is observed near the wall but far away from the wall entropy generation decreases rapidly. The effect of the temperature ratio parameter on entropy generation is displayed in Fig. 24. It is clearly seen from this figure that entropy generation is decreases when the temperature ratio parameter enhances. Dispersion of magnetic parameter on entropy generation is displayed in Fig. 25. Magnetic parameters persuade Lorentz force which boosts the entropy generation. Fig. 26 exhibits the influence of the unsteady parameter, which decays the entropy generation. The effect of Brickman number is displayed in Fig. 27. Brickman number produced heat transport by viscous heating, which makes an improvement in entropy generation. Variation of entropy generation with Reynolds number is shown in Fig. 28. It is noted that entropy generation rises with larger Reynolds numbers because larger Reynolds numbers correspond to larger inertia and smaller viscous force.

Tables 1-3 include the numerical values of skin friction coefficient, local Nusselt number and Sherwood number. The magnitude of the skin friction coefficient decreases for larger values of R , G , ϵ and Ec . However, it increases when We , α and Pr are increased. It is noticed that the heat transfer at the wall $-\theta(0)$ increases for larger values of ϵ , G , Bi and it decreases for larger We , α , R and Ec . Table 2 shows that the local Sherwood number increases when radiation parameter R and Schmidt number Sc are increased.

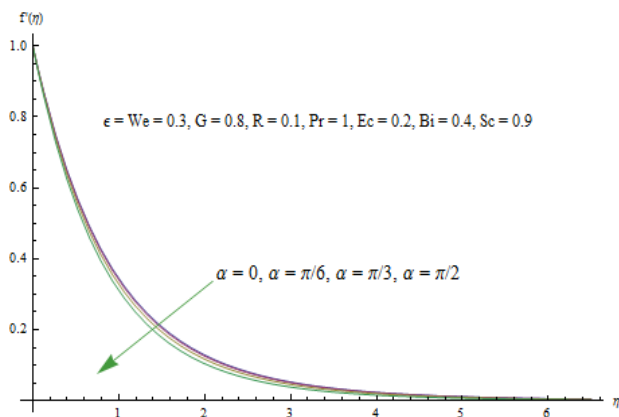


Fig. 4. Influence of α on $f'(\eta)$.

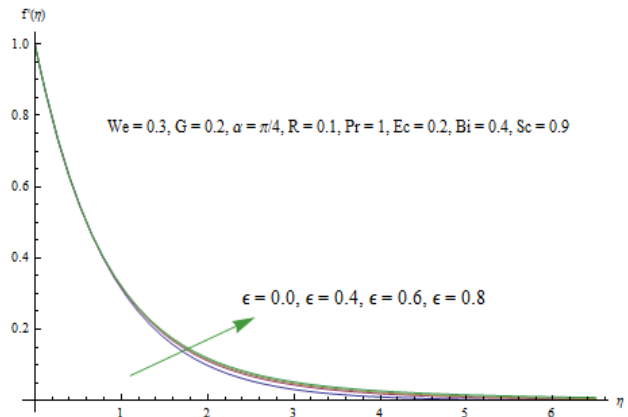


Fig. 5. Influence of ϵ on $f'(\eta)$.

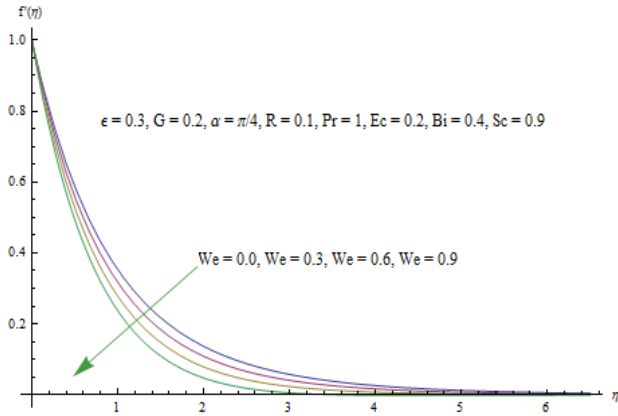


Fig. 6. Influence of We on $f'(\eta)$.

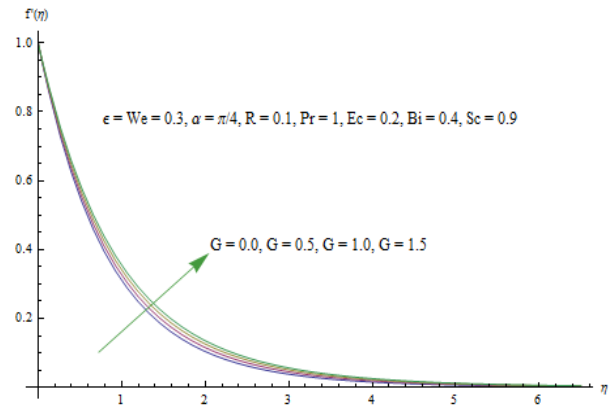


Fig. 7. Influence of Go on $f'(\eta)$.

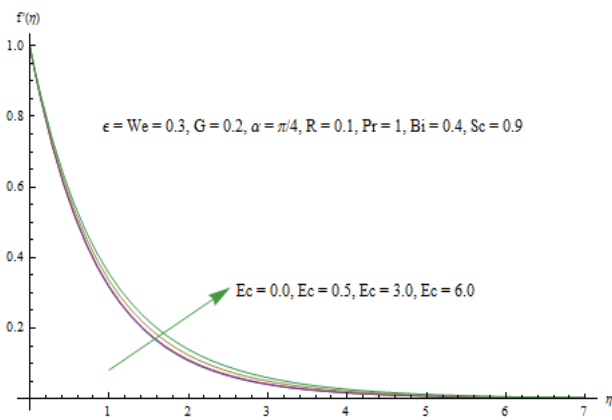


Fig. 8. Influence of Ec on $f'(\eta)$.

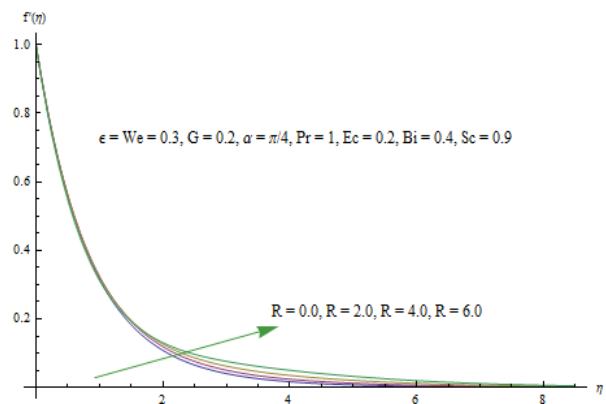


Fig. 9. Influence of R on $f'(\eta)$.

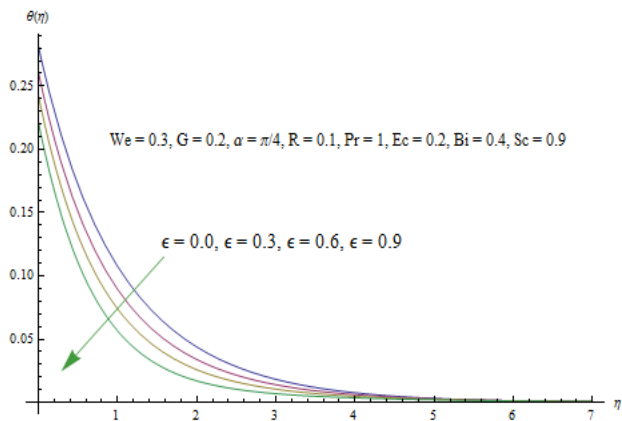


Fig. 10. Influence of ϵ on $\eta(\theta)$.

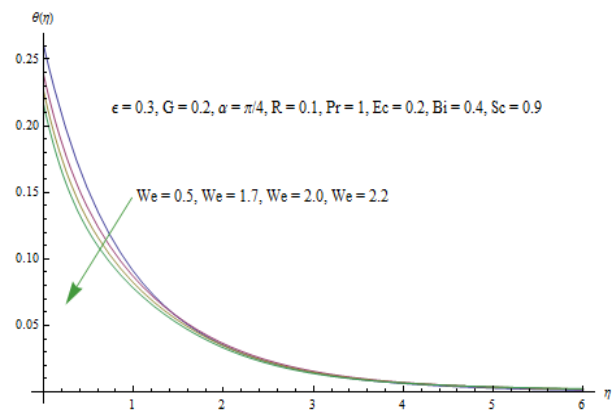


Fig. 11. Influence of We on $\eta(f)$.

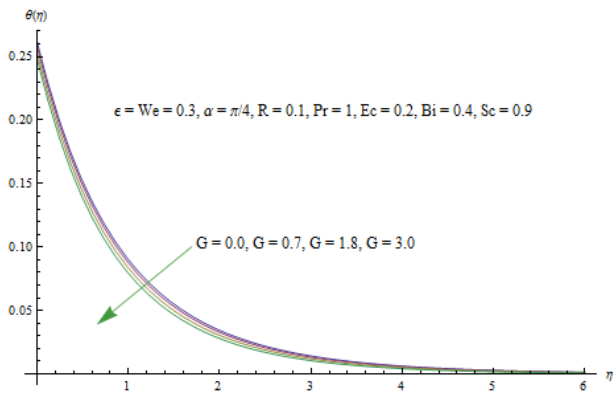


Fig. 12. Influence of G on $\eta(\theta)$.

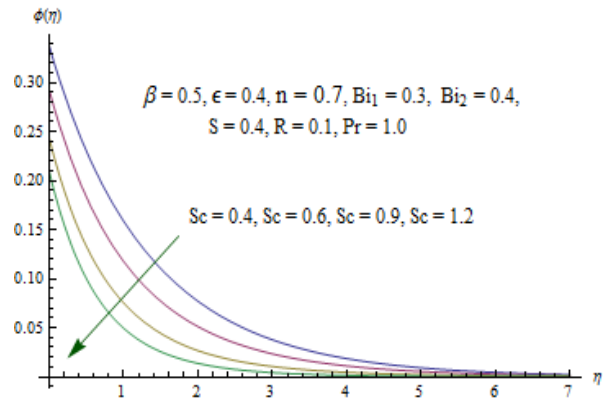


Fig. 13. Influence of α on $\eta(\theta)$.

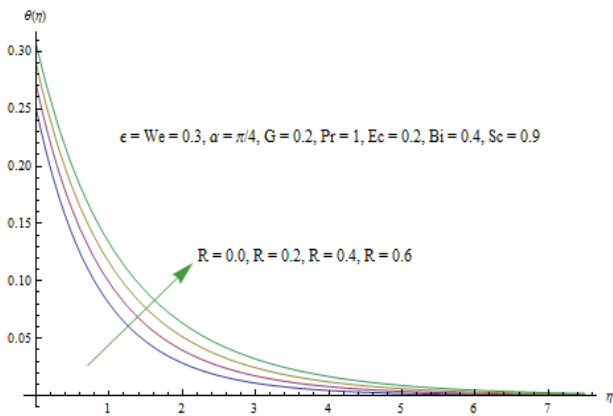


Fig. 14. Influence of R on $\eta(\theta)$.

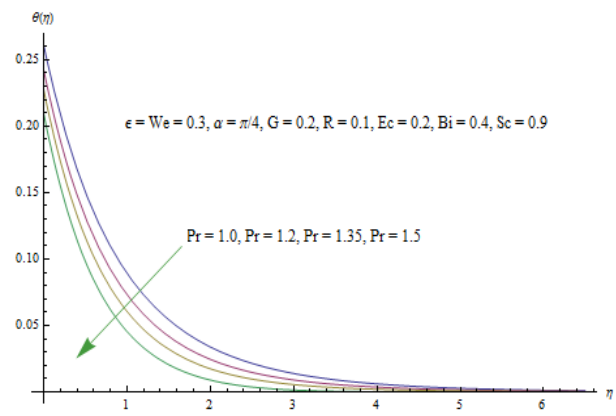


Fig. 15. Influence of Pr on $\eta(\theta)$.

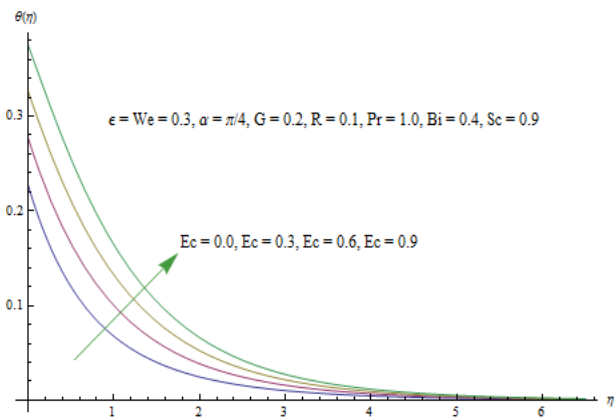


Fig. 16. Influence of Ec on $\eta(\theta)$.

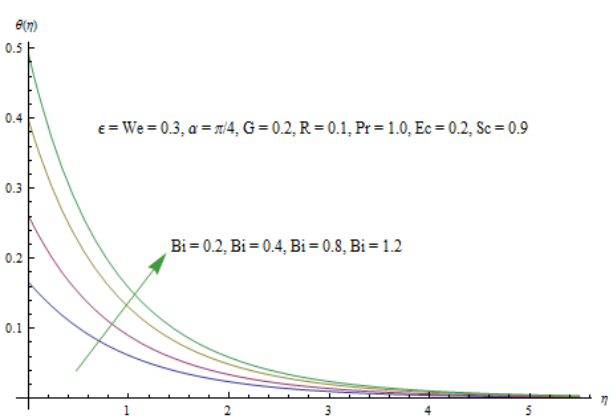


Fig. 17. Influence of Bi on $\eta(\theta)$.

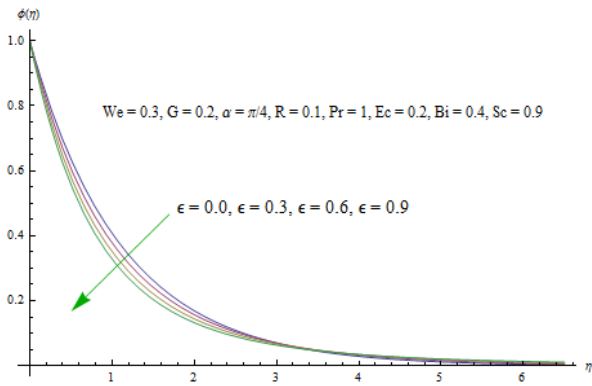


Fig. 18. Influence of ϵ on $\eta(\phi)$.

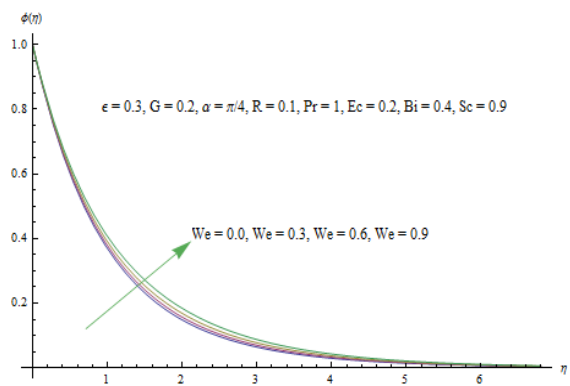


Fig. 19. Influence of We on $\eta(\phi)$.

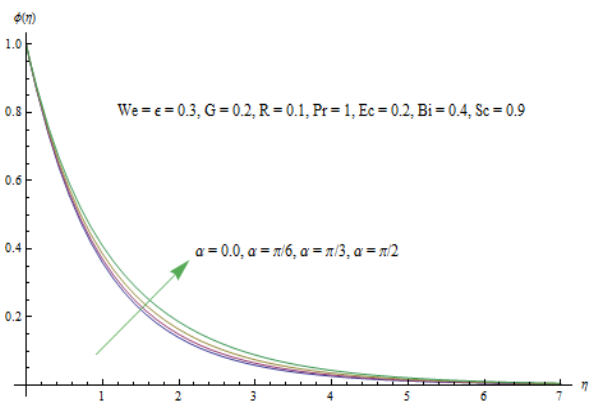


Fig. 20. Influence of α on $\eta(\phi)$.

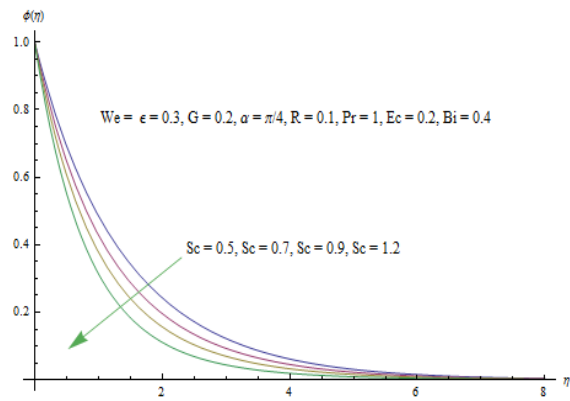


Fig. 21. Influence of Sc on $\eta(\phi)$.

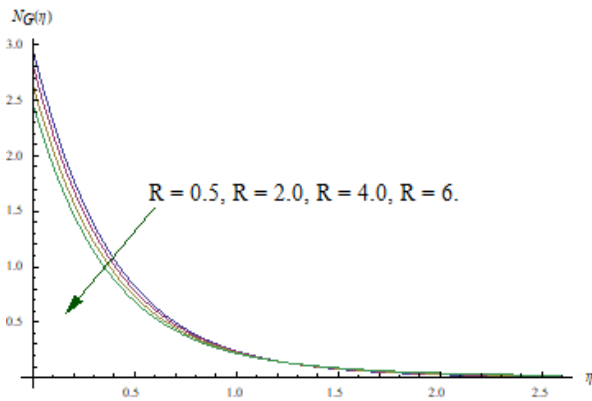


Fig. 22. Influence of R on $N_G(\eta)$.

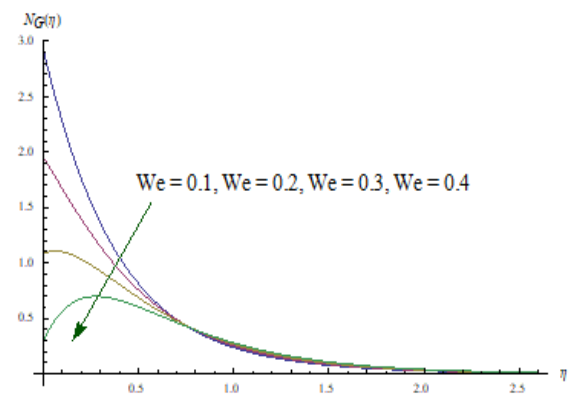


Fig. 23. Influence of We on $N_G(\eta)$.

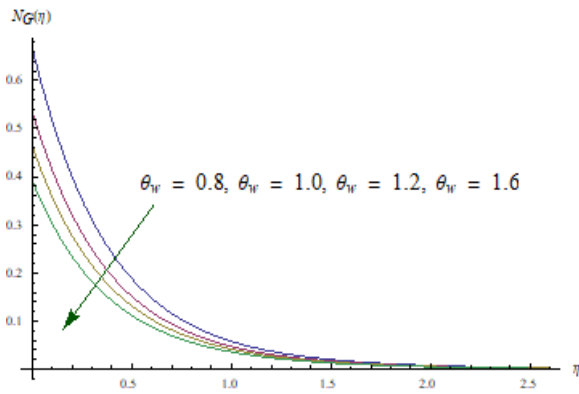


Fig. 24. Influence of θ_{∞} on $N_G(\eta)$.

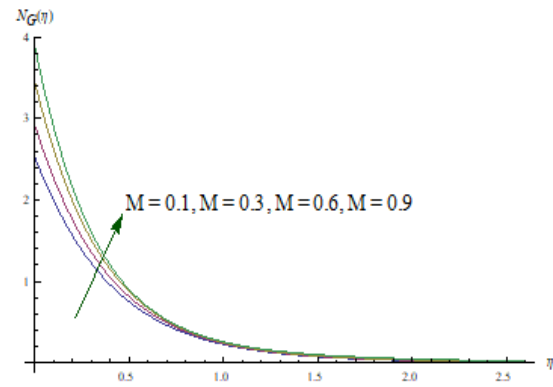


Fig. 25. Influence of M on $N_G(\eta)$.

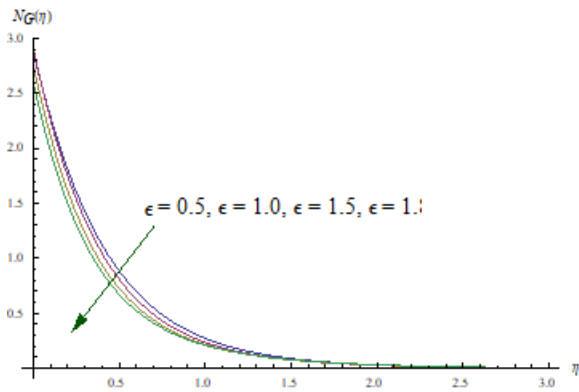


Fig. 26. Influence of ϵ on $N_G(\eta)$.

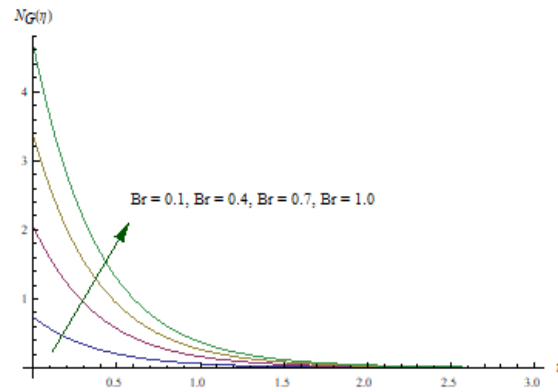


Fig. 27. Influence of Br on $N_G(\eta)$.

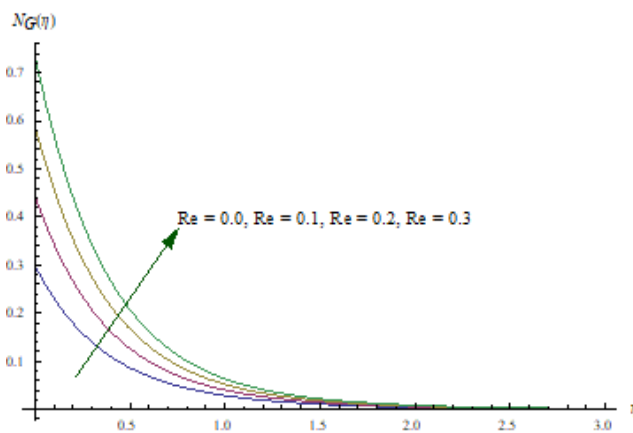


Fig. 28. Influence of Re on $N_G(\eta)$.

Table 1. Values of skin friction coefficient $Re_x^{1/2} C_f$ for the parameters ε , We , G , α , R , Pr , E_c , and Bi

ε	We	G	α	R	Pr	E_c	Bi	$-\frac{1}{2}Re_x^{1/2}C_f$
0.0	0.3	0.2	$\pi/4$	0.1	1.0	0.2	0.4	2.22135
	0.2							2.13488
	0.4							2.04054
0.3	0.0							1.08510
	0.2							1.73555
	0.4							2.46015
	0.3	0.0						2.12112
		0.2						2.08842
		0.4						2.05607
			0.0					2.07498
			$\pi/6$					2.08112
			$\pi/3$					2.09796
				0.0				2.09047
				0.3				2.08459
				0.6				2.07940
					0.5			2.07403
					0.9			2.08657
					1.1			2.08999
						0.0		2.09390
						0.3		2.08569
						0.6		2.07760
							0.2	2.09969
							0.6	2.07946
							1.0	2.06611

Table 2. Values of local Nusselt number $Nu/Re_x^{1/2}$ for the parameters ε , We , G , α , R , Pr , E_c , E_c and Bi

ε	We	G	α	R	Pr	E_c	Bi	$-\left(1 + \frac{4}{3}R\right)\theta'(0)$
0.0	0.3	0.2	$\pi/4$	0.1	1.0	0.2	0.4	0.286182
	0.3							0.295144
	0.6							0.301292
0.3	0.0							0.295985
	0.2							0.295379
	0.5							0.294885
		0.0						0.294608
		0.3						0.295403
		0.5						0.295907
			0.0					0.295359
			$\pi/6$					0.295261
			$\pi/3$					0.294989
				0.0				0.299395
				0.1				0.295144
				0.3				0.287178
					0.7			0.281292
					1.1			0.298509
					1.4			0.306404
						0.0		0.308526
						0.2		0.295144
						0.6		0.268771
							0.2	0.166532
							0.5	0.349078
							0.9	0.517163

Table 3. Values of local Sherwood number Sh for the parameters R , We , α and Sc .

R	We	α	Sc	$-\phi'(0)$
0.0				0.94588
0.3				0.94707
0.9				0.94930
	0.0			0.96707
	0.2			0.95358
	0.3			0.94628
		0.0		0.94783
		$\pi/6$		0.94713
		$\pi/4$		0.94628
			$\pi/40.7$	0.87195
			0.9	0.94628
			1.1	1.14703

Main points

Boundary layer flow of MHD Walters' B liquid by an inclined stretching sheet is discussed in the presence of viscous dissipation and thermal radiation. The main observations are mentioned below:

- Velocity field $f'(\eta)$ is a decreasing function of parameter ε .
- Effects of ε on the temperature and concentration fields are qualitatively similar.
- Weissenberg number We decreases both the velocity and associated boundary layer thickness. Visible number contains viscoelasticity that produces tensile stress which contracts the boundary layer and consequently velocity decreases.
- Weissenberg number We increases the temperature and concentration fields. Velocity field f' is a decreasing function through larger α . On the other hand, when \rightarrow changes from 0 to 2, i.e. when the sheet moves from vertical to horizontal direction, the strength of buoyancy force decreases and consequently the velocity and the boundary layer thickness decrease. Effects of Ec , G and R on velocity field are qualitatively similar. Physically this is because of increase in radiation parameter P , the rate of radiative heat transfer to the fluid increases. For Eckert number the kinetic energy increases by increasing Ec and so the temperature profile increases.
- From physical point of view, the larger Prandtl number coincides with the weaker thermal diffusivity and thinner boundary layer. This is because a higher Prandtl number fluid has a relatively lower thermal conductivity which reduces conduction and thereby increases the variation of thermal characteristics. There is an enhancement of

temperature for larger values of Eckert number Ec , thermal radiation R and Biot number Bi . It is due to the reason that stronger convective heating rises the temperature and thermal boundary layer thickness.

- Variations of ε and Sc on the concentration field are qualitatively similar.
- For a larger Schmidt number viscosity increases and concentration decreases.
- Magnitude of skin friction coefficient is a decreasing function of α , We , Ec and R .
- Influences of ε , G and Bi on the temperature gradient at the surface are qualitatively similar.
- The temperature gradient at the surface decreases when We , Ec and R are enhanced.
- Entropy generation boosts up with magnetic parameter, Reynolds number and Brinkman number, while the reverse behavior is observed for larger values of radiation parameter, temperature ratio parameter, unsteady parameter, and Weissenberg number.

Conflict of interest: There is no conflict of interest.

REFERENCES

1. M. R. Krishnamurthy, B. C. Prasannakumara, B. J. Gireesha, R. S. R. Gorla, *Eng. Sci. Tech., Int. J.*, **19**, 53 (2016).
2. N. Balazadeh, M. Sheikholeslami, D. D. Ganji, Z. Li, *J. Molec. Liqs.*, **260**, 30 (2019).
3. T. Hayat, A. Qayyum, F. Alsaadi, M. Awais, A. M. Dobaie, *European Phys. J. Plus*, **128**, 85 (2013).
4. C. Fetecau, A. M. Imran, A. Sohail, *Ann. Acad. Rom. Sci. Ser. Math. Appl.*, **6**, 74 (2014).
5. C. Fetecau, M. Rana, N. Nigar, C. Fetecau, *ZNA Physical Sci.*, **69**, 232 (2014).
6. M. Turkyilmazoglu, *Int. J. Mech. Sci.*, **77**, 263 (2013).
7. R. Ellahi, *Appl. Math. Modell.*, **37**, 1451 (2013).
8. M. Waqas, S. A. Shehzad, T. Hayat, M. I. Khan, A.

- Alsaedi, *J. Phys. Chem. Solids*, **133**, 45 (2019).
9. T. Hayat, S. Asad, M. Qasim, A. A. Hendi, *Int. J. Num. Meth. Fluid*, **69**, 1350 (2012).
 10. M. M. Rashidi, M. Ali, N. Freidoonimehr, B. Rostami, A. Hossian, *Adv. Mech. Eng.* **2014**, 10 (2014).
 11. T. Hayat, M. Mustafa, S. Asghar, *Nonlinear Analysis: Real World Appl.*, **11**, 3186 (2010).
 12. S. Mukhopadhyay, K. Bhattacharyya, *J. Egyptian Math. Soc.*, **12**, 229 (2012).
 13. S. Mukhopadhyay, P. Ranjan De, K. Bhattacharyya, G. C. Layek, *Ain Shams Eng. J.*, **4**, 933 (2013).
 14. K. Bhattacharyya, *Ain Shams Eng. J.*, **4**, 259 (2013).
 15. T. Hayat, S. Asad, M. Mustafa, A. Alsaedi, *Computer Fluid*, **108**, 179 (2015).
 16. A. Bejan, Entropy generation minimization, New York, CRC press, 1996.
 17. A. Bejan, Entropy generation through heat and fluid flow, Wiley, 1982.
 18. M. M. Rashidi, S. Bagheri, E. Mamoniati, N. Freidoonimeh, *Ain Shams Eng. J.*, **8**, 77 (2017).
 19. H. Sithole, H. Mondal, P. Sibanda, *Result in Physics*, **9**, 1077 (2018).
 20. R. Naz, M. Noor, T. Hayat, M. Javed, A. Alsaedi, *Comm. Heat Mass Transfer*, **110**, 104431 (2020).
 21. M. Turkyilmazoglu, *Int. J. Therm. Sci.*, **50**, 88 (2011).
 22. M. Turkyilmazoglu, *J. Heat Transfer*, **137**, 71701 (2012).
 23. M. Turkyilmazoglu, *Applied Math. Modell.*, **71**, 1 (2019).
 24. B. J. Akinbo, B. I. Olajuwon, *Int. Commun. Heat Mass Transfer*, **121**, 105115 (2021).
 25. M. I. Khan, M. Waqas, T. Hayat, A. Alsaedi, M. I. Khan, *Int. J. Hydrogen Energy*, **42**, 26408 (2017).
 26. M. Turkyilmazoglu, *Int. J. Thermal Sci.*, **50**, 2264 (2011).